Int. J. Electrochem. Sci., 12 **(2017)** 9445 – 9455, doi: 10.20964/2017.10.40

International Journal of
ELECTROCHEMICAL
SCIENCE
www.electrochemsci.org

Short Communication

The Corrosion Behavior of 17-4 Stainless Steel in a Stainless Steel-Carbon Steel Galvanic Couple

Longjun Chen, Junying Hu[*]*, Xiankang Zhong, Siyu Yu, Zhi Zhang, Dezhi Zeng, Taihe Shi*

State Key Laboratory of Oil and Gas Reservoir Geology and Exploitation, College of Petroleum Engineering, Southwest Petroleum University, Chengdu 610500, China
[*]E-mail: hujunying01@yeah.net

Received: 16 June 2017 / *Accepted:* 4 August 2017 / *Published:* 12 September 2017

In this work, the corrosion behavior of 17-4 stainless steel in a stainless steel (17-4) and carbon steel (C110) galvanic couple was investigated using electrochemical methods including open circuit potential, galvanic potential, electrochemical impedance spectroscopy and Mott-Schottky curves. The results show that the corrosion resistance of 17-4 stainless steel decreases, although it is generally considered that stainless steel acting as the cathode in this kind of galvanic couple should be protected. This can be attributed to that the passive film on the 17-4 stainless steel is destabilized by the cathodic polarization in this galvanic couple. Consequently, a decrease in corrosion resistance of 17-4 stainless steel can be found.

Keywords: Galvanic corrosion; Stainless steel; Carbon steel; Electrochemical measurement

1. INTRODUCTION

Normally, the corrosion of the more noble metal would decrease, the corrosion of the less noble metal would increase, when two dissimilar metals contact with each other in an electrolyte. The phenomenon is called as dissimilar-metal contact or galvanic corrosion 0. Furthermore, there are always different metals contact, such as pipeline and heat exchanger, due to the mechanical property, total cost, special demand and so on 2. The stainless steel and carbon steel may be directly connected through a thread or collar in industry such as oil and gas field. Therefore, it is of great interest and importance to understand the galvanic corrosion between stainless steel and carbon steel.

Extensive work about the galvanic corrosion between stainless steel and carbon steel has been conducted in different environments [3-13]. For example, Ren et al. 3 has studied the galvanic corrosion of casing pipe joint (17-4) -C110 couple in 13.2 g/L NaCl. It was found that higher galvanic

corrosion would occur when temperature increases from 40℃ to 80℃, and the galvanic effect is about 2.58 when samples in brine water containing H_2S and CO_2 at 40℃ and 20 MPa. Moreover, the galvanic effect is mitigated if the two-metal is placed in vapor. However, most of these work focused on the corrosion of carbon steel in stainless steel and carbon steel couple (SC couple). The corrosion behavior of stainless steel is missing, because it is generally considered that in a SC couple the carbon steel acts as an anode and the stainless steel acts as a cathode. In this case, the stainless steel is usually protected and therefore no corrosion needs to be considered.

The passive film on the stainless steel plays a significant role in its corrosion resistan ce. In a SC couple, the passive film may be affected because there is a cathodic polarization on the stainless surface once the stainless steel is connected with the carbon steel in the electrolyte. In this case, the corrosion resistance may be greatly changed. Accordingly, it is of great significance to study the corrosion behavior of stainless steel in a SC couple.

Electrochemical techniques are usually considered as the efficient and reliable ways to investigate the corrosion behaviors and mechanisms of metal and alloys [14-16]. In this work, the corrosion behavior of 17-4 stainless steel in a SC couple in formation water was investigated using electrochemical measurements (open circuit potential, galvanic potential, electrochemical impedance spectroscopy and Mott-Schottky curves).

2. EXPERIMENTAL

The materials used in this work were 17-4 stainless steel and C110 carbon steel, with the compositions listed in Table 1. The steel electrodes were machined into two sizes: (1) large samples of 10×10×3 mm and (2) small samples of 5×4×3 mm. It is important to note that small samples only were used to test galvanic potential of (17-4)-C110 couples at Sc:Sa (cathode/anode area ratio)=1:5 and Sc:Sa=5:1 in Section 3.1. The samples were sealed in epoxy resin, leaving a fixed area of steel surface (1 cm^2 and 0.2 cm^2 for large samples and small samples, respectively) exposed to the solution. A copper wire was welded to the backside of the electrode to ensure the electrical contact. Prior to experiments, the electrode surface was grounded using sand paper with 400 and 800 grit numbers, sequentially, and then rinsed with distilled water and cleaned in an ultrasonic bath with ethanol. Specimens then were taken out and dried by nitrogen gas and immediately used for testing.

Table 1. Chemical compositions (wt. %) of steels used in this work.

Steels	Ni	Cr	C	Si	Mn	P	S	Mo	Cu	Nb	Fe
17-4	3.83	16.20	0.07	0.77	0.64	0.03	0.03	-	2.32	0.56	Balance
C110	0.04	-	0.27	0.26	0.48	-	-	0.72	0.11	-	Balance

The test solution was prepared with analytical grade regents and distilled water according to the composition of formation water produced along with natural gas from the gas field in Southwest China. It was composed of 17.24 g/L NaCl, 10.54 g/L KCl, 0.45g/L $CaCl_2$, 0.37g/L Na_2SO_4, 0.5 g/L

$MgCl_2$•$6H_2O$ and 3.98g/L $NaHCO_3$. The solution was deoxygenated with a continuous CO_2 gas flow purge. Two hours later, put the specimen into the solution. CO_2 gas purging was maintained to ensure an entire saturation and stop the O_2 from entering. After saturated with CO_2, the pH of solution is 6.13. The temperature for all the tests in this work was maintained at 25 ± 0.5℃.

To ensure the reproducibility, each type of electrochemical measurements was repeated at least three times. The electrochemical tests, including open circuit potential (OCP), galvanic potential, electrochemical impedance spectroscopy (EIS) and Mott-Schottky, were conducted using a CS 350 electrochemical workstation (Wuhan Corrtest Instruments Corp. Ltd., China). A four-electrode electrochemical cell was used for galvanic potential test where C110 carbon steel was used as working electrode 1 (WE1), 17-4 stainless steel was used as working electrode 2 (WE2), a platinum plate was used as a counter electrode and a saturated calomel electrode (SCE) was used as a reference electrode. The OCP of the uncoupled specimens and galvanic potential of the coupled specimens were continuously recorded during the whole tests. EIS measurements were performed using classical three-electrode configuration at OCP with a sinusoidal potential perturbation of 10 mV (peak to peak) in the frequency range from 100 kHz to 10 mHz. It should be pointed out that the EIS measurement of the electrode in the galvanic couple was conducted after disconnecting electrical contact of the couple. To investigate the properties of passive film on 17-4 stainless steel, Mott-Schottky curves of 17-4 stainless steel were measured in CO_2 purged formation water. Mott-Schottky tests were performed by shifting the potential from -0.6V (vs. OCP) to +0.5V (vs. OCP) with a scanning rate of 1 mV per step at 1 kHz.

3. RESULTS AND DISCUSSION

3.1. Potential

The OCP of 17-4 stainless steel and C110 carbon steel in CO_2 purged formation water are shown in Figure 1. It is seen that the OCP of 17-4 stainless steel increases sharply at the very beginning, and then slowly increases with time. After about 15000 s, the OCP does not change significantly any more. The increase in potential could be ascribed to the formation of a passive film on the 17-4 stainless steel surface. The OCP of 17-4 stainless steel would keep close to a constant value when there is a balance of formation and dissolution of the passive film on 17-4 stainless steel. In contrast, the OCP of C110 carbon steel always keeps near a constant value (-0.731 V vs. SCE) which is more negative than 17-4 stainless steel. These results definitely indicate that 17-4 stainless steel acts as a cathode and C110 carbon steel acts as an anode in the (17-4)-C110 couple in CO_2 purged formation water at 25 ℃. More importantly, the potential difference between C110 carbon steel and 17-4 stainless steel is relatively large. For example, the potential difference at 15000 s between these two steels is about 0.473 V which is a very strong driving force of galvanic corrosion. According to the literature, a serious galvanic corrosion will occur if the potential difference between both metals excesses a critical value of 0.25 V 17. Therefore, it is expected that a remarkable galvanic corrosion between C110 carbon steel and 17-4 stainless steel could occur in the present work.

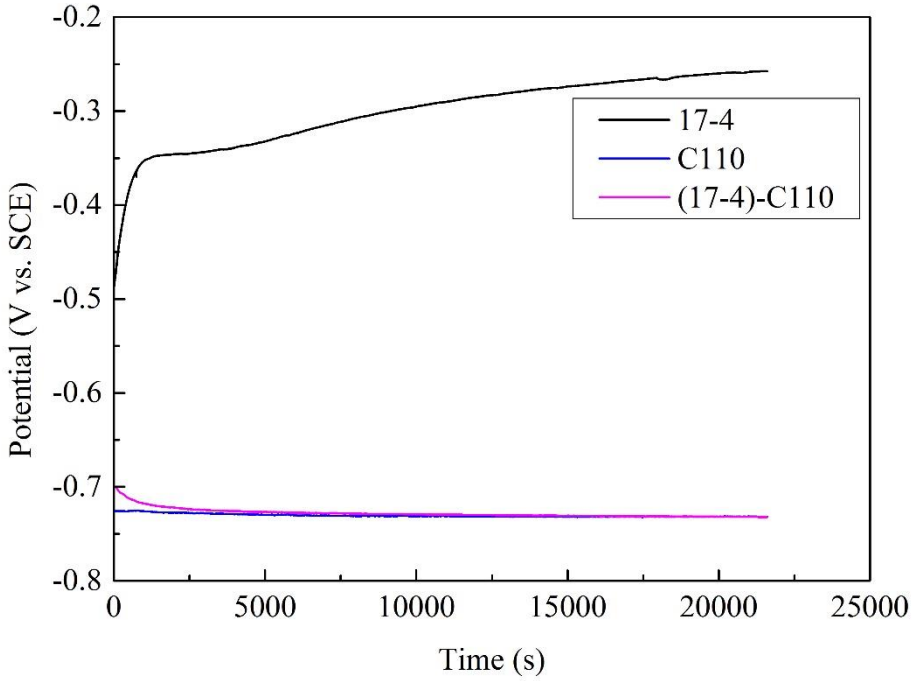

Figure 1. Corrosion potential as a function of time of the samples in CO_2 purged formation water at 25℃ and initial pH 6.13.

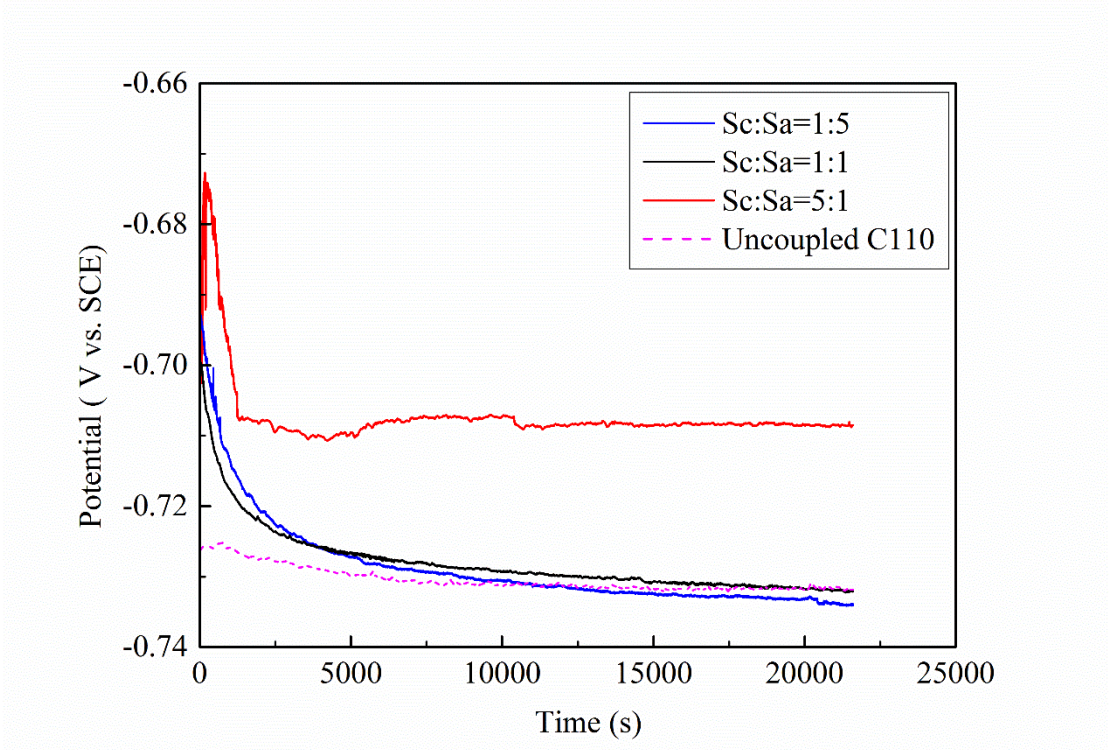

Figure 2. Galvanic potential as a function of time of uncoupled C110 carbon steel and (17-4)-C110 couples at various cathode/ anode area ratio (Sc:Sa) in CO_2 purged formation water at 25℃ and initial pH 6.13.

The galvanic potential of (17-4)-C110 couple in CO_2 purged formation water is also shown in Figure 1. At the very beginning, the galvanic potential is located at about -0.700 V vs. SCE, then decreases rapidly with time and finally reaches a stable value where the potential vs. time curves is almost overlapping with that of C110 carbon steel. It is interesting that the final galvanic potential is so close to the OCP of C110 carbon steel.

According to the classic mixed potential theory, the galvanic potential should be located between the potential of 17-4 stainless steel and the potential of C110 carbon steel. It is indeed true for the galvanic potential at the very beginning when the two electrodes are connected. However, the stable galvanic potential of (17-4)-C110 couple approximates the potential of anode sample C110 carbon steel. For that situation, it can be assumed that 17-4 stainless steel suffered cathodic polarization, which destabilizes the passive layer of the 17-4 stainless steel, resulting in a decrease in corrosion potential of 17-4 stainless steel 18. That's why the galvanic potential decreases with time and then keeps at a stable value which is very close to the potential of C110 carbon steel.

To further investigate the effect of cathodic polarization on the passive film, galvanic potential of (17-4)-C110 couple at various cathode/ anode area ratios in CO_2 purged formation water were studied, as shown in Figure 2. It reveals that the galvanic potential increases with increasing cathode/ anode area ratio. For example, the galvanic potential of (17-4)-C110 couple at Sc:Sa=1:5 is slightly lower than the OCP of C110 carbon steel. With the cathode/anode area ratio increasing to 5:1, the galvanic potential is considerably higher than that when the cathode/anode area ration is 1:1. This indicates that a bigger cathodic area is benefit for preventing the passive film on 17-4 stainless steel from destabilization.

3.2. Electrochemical impedance spectroscopy

The EIS results of uncoupled 17-4 stainless steel in CO_2 purged formation water are shown in Figure 3. The variation in the diameter of Nyquist plots decreases with immersed time, the impedance of 17-4 stainless steel at 1h is relatively small. After 6h, the change in the impedance of 17-4 stainless steel is much small. It can be ascribed that passive film generates and grows on stainless steel at initial stage. At 6h, the passive film reaches relatively stable stage, changing to thicker, denser and more protective.

Figure 4 shows the EIS results of 17-4 stainless steel coupled with C110 carbon steel in CO_2 purged formation water. Obviously, the diameter of Nyquist plot decreases over time. Compared to uncoupled 17-4 stainless steel, as shown in Figure 3, the impedance of coupled 17-4 stainless steel is much smaller, which means coupled 17-4 stainless steel shows a smaller corrosion resistance. The galvanic effect on 17-4 stainless steel (acting as cathode) is much apparent, which is inconsistent with the early cognition of galvanic corrosion **Error! Reference source not found.** . It can be contributed to the cathodic polarization and the destabilization of passive film on 17-4 stainless steel surface.

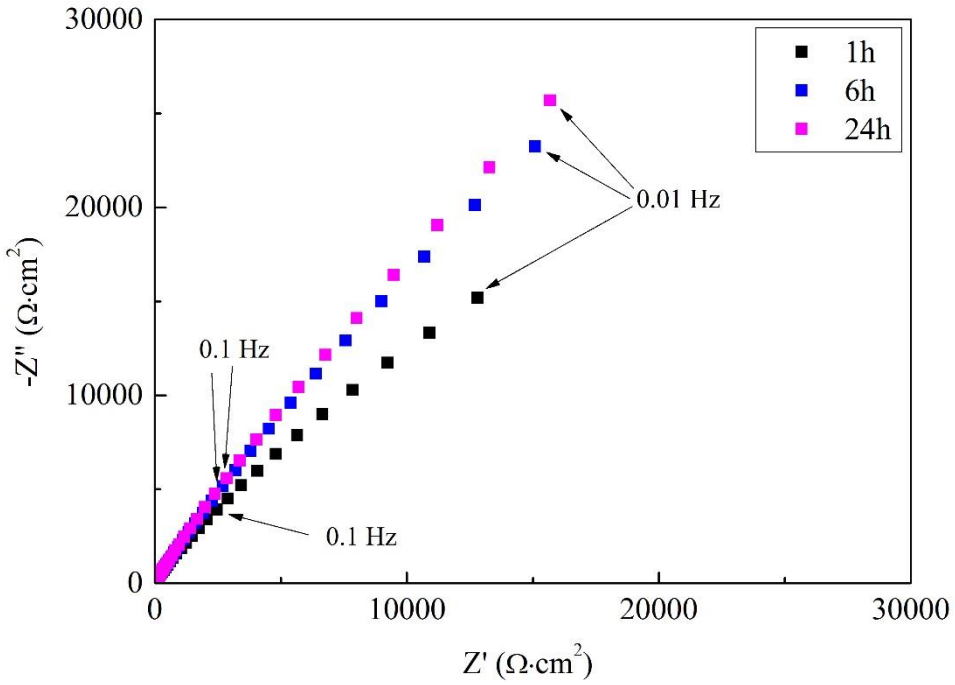

Figure 3. EIS results of the uncoupled 17-4 stainless steel in CO_2 purged formation water at 25℃ and initial pH 6.13.

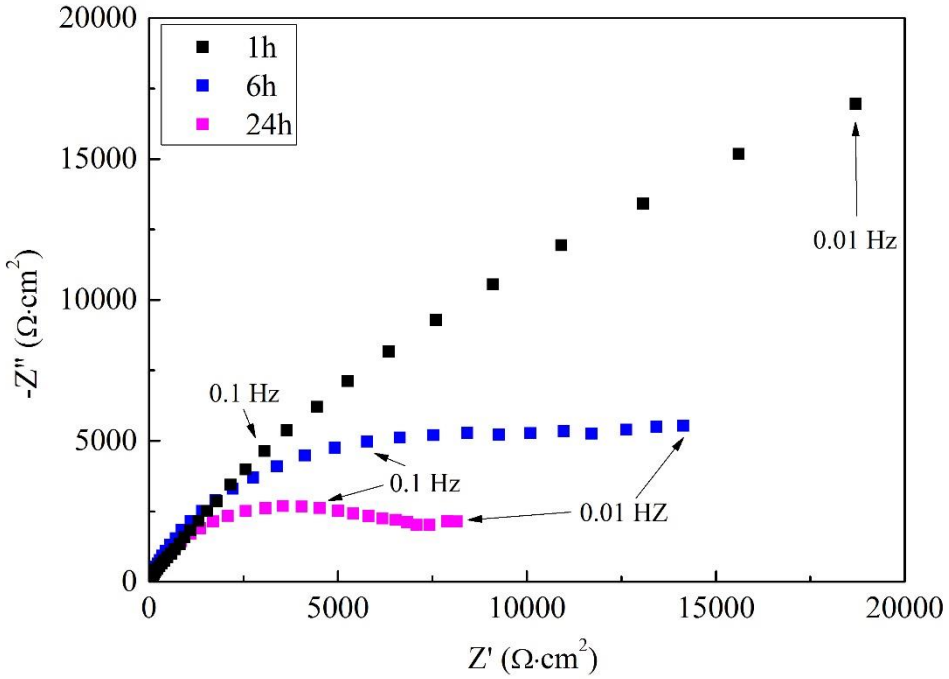

Figure 4. EIS results of the coupled 17-4 stainless steel in CO_2 purged formation water at 25℃ and initial pH 6.13.

In order to demonstrate the results of EIS of coupled 17-4 stainless steel, the EIS experiments of the 17-4 stainless steel polarized at different cathodic potentials for 6h were also measured, the results are shown in Figure 5. Apparently, the diameter of Ntquist plot of 17-4 stainless steel decreases with the increasing strength of cathodic polarization. As presented in Figure 1, the distinction of OCP between C110 carbon steel and 17-4 stainless steel in deoxygenized formation water is about 0.47 V, so the EIS data of 17-4 stainless steel polarized at -0.5 V vs. OCP should be similar to that of coupled 17-4 stainless steel. It is really true that these two diameters of Nyquist plots are very close to each other, as shown in Figures 4 and 5. The experiments demonstrate that in the (17-4)-C110 couple, 17-4 stainless steel acted as cathode where the cathodic polarization can result in the destabilization of the passive film. Consequently, the corrosion resistance of 17-4 stainless steel decreases in this galvanic couple.

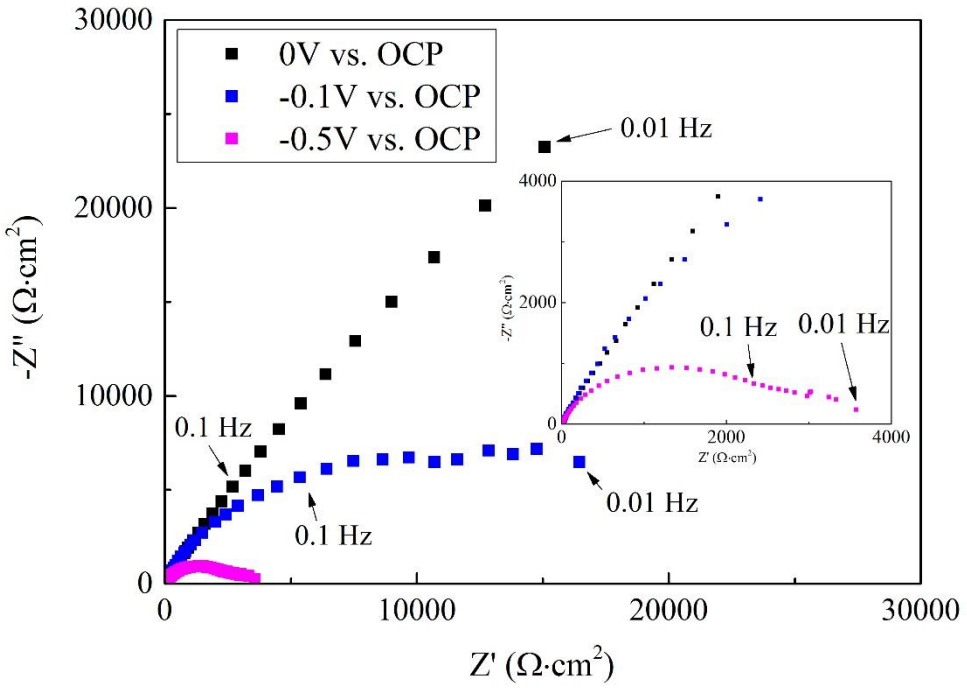

Figure 5. EIS results of the 17-4 stainless steel polarized at different potentials in CO_2 purged formation water at 25℃ and initial pH 6.13.

3.3. Mott-Schottky curves

The Mott-Schottky curves describe the C_{sc}^{-2} as a function of the potential becomes to 20:

For n type semiconductor $$\frac{1}{C_{sc}^{2}}=\frac{2}{\varepsilon\varepsilon_0 eN_D}\left(E-E_{fb}-\frac{kT}{e}\right) \quad (1)$$

For p type semiconductor $$\frac{1}{C_{sc}^{2}}=\frac{-2}{\varepsilon\varepsilon_0 eN_A}\left(E-E_{fb}-\frac{kT}{e}\right) \quad (2)$$

Where C_{sc} is the space-charge capacitance, N_D and N_A are donor and accepter densities (cm^{-3}), e is the electron charge, ε is the dielectric constant of iron oxide (ε=12 21), ε_0 is the vacuum

permittivity (8.854×10^{-14} F/cm), k is the Boltzmann constant (1.38×10^{-23} J/K), T is the absolute temperature and E_{fb} is the flat band potential.

Generally, the space-charge capacitance C_{sc} is substituted by the capacitance of the film-electrolyte interface C, which could be described by the following equations 22, 23]:

$$\frac{1}{C}=\frac{1}{C_{sc}}+\frac{1}{C_H} \qquad (3)$$

Where C_H is the Helmholtz capacitance. However, at high frequency, such as 1 kHz used in this paper, C is mainly expressed as C_{SC}, due to the Helmholtz capacitance is negligible 24. The interfacial capacitance C is obtained from equation (4).

$$C=-\frac{1}{2\pi fZ''} \qquad (4)$$

Where Z'' is the imaginary component of the impedance and f is the scan frequency.

The results of Mott-Schottky test of 17-4 stainless steel are shown in Figure 6, which is similar to Liz Pons 25. In the potential range of -1.1 V to -0.3 V, it plays p-type semiconductor on the basis of positive slope and presents two linear regions. C_{sc}^{-2} decreases with potential increasing at first stage, due to the ionization of deep acceptor 26. However, an obvious shift occurs at -0.82V, the slope of the curve increases with the increasing potential. But n-type semiconductor is exhibited in higher potential range.

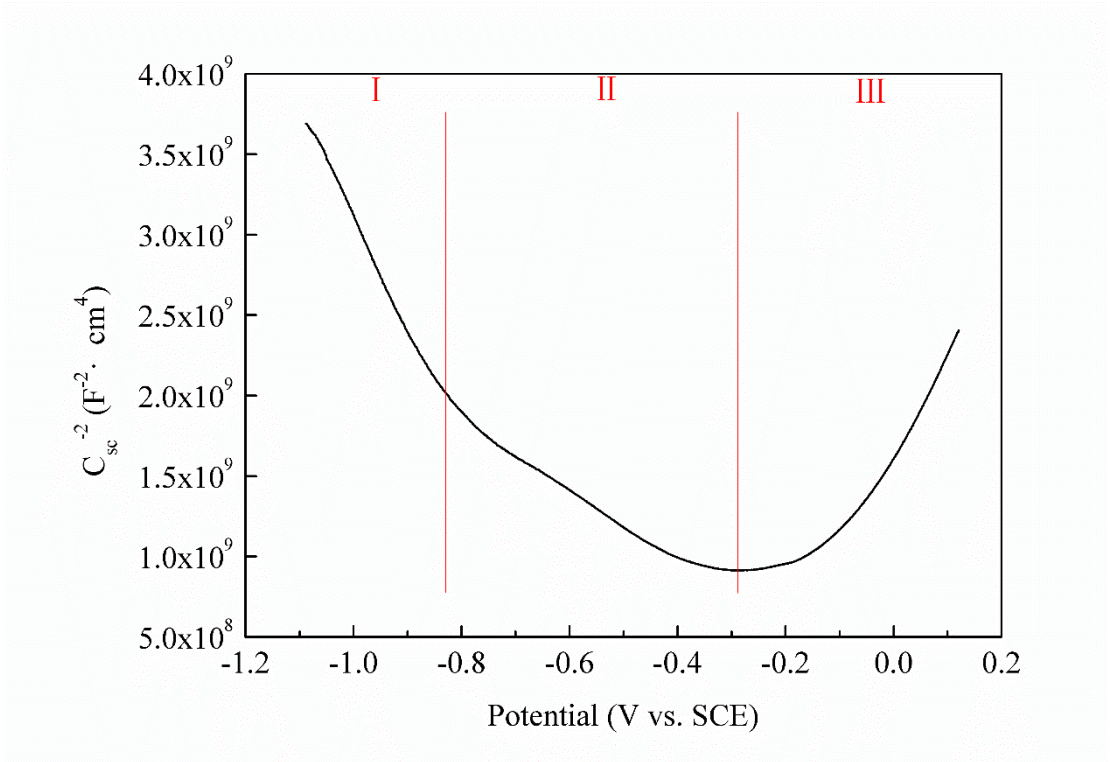

Figure 6. The Mott-Schottky plot of passive film on 17-4 stainless steel in CO_2 purged formation water at 25℃ and initial pH 6.13.

The bi-layer structure could attribute to obvious difference layers, the inner layer rich in chromium oxide (Cr_2O_3), acting as p-type semiconductor and the outer layer mainly containing iron oxides (Fe_2O_3) and hydroxides ($Fe(OH)_3$), performing as n-type semiconductor 26. Based on the factors above, the deep acceptor density N_{A2} and shallow acceptor density N_{A1} should be separated, and evaluated by following relationship 27:

For region II $$S_{\text{II}} = -\frac{2}{\varepsilon\varepsilon_0 e N_{A1}} \quad (5)$$

For region I $$S_{\text{I}} = -\frac{2}{\varepsilon\varepsilon_0 e\left(N_{A1}+N_{A2}\right)} \quad (6)$$

The value of N_D, N_{A1} and N_{A2} are calculated and listed in Table 2.

Table 2. Charge carrier densities in passive film on 17-4 stainless steel in CO_2 purged formation water at 25℃ and initial pH 6.13.

N_D ,cm^{-3}	N_{A1} ,cm^{-3}	N_{A2} ,cm^{-3}
1.853×10^{21}	5.307×10^{21}	1.794×10^{21}

Due to the galvanic potential is about -0.73V, region I would not be discussed in detail. According to the results of Hakiki 28, the response of capacitance, as region II, controlled by electron of inner layer mainly containing chromium oxide. Meanwhile, the spaced charge layer of chromium oxide in the run out of state, the one of iron oxide in an enrich state that equal to conductor. Consequently, the distance between excess electron in the passive film and solution electron is much short, and the film formed on 17-4 stainless steel presents as p-type semiconductor for the p-type semiconductor character of chromium oxide 28. However, the region III acts as n-type semiconductor, mostly controlled by iron oxide and hydroxides, and the space charge condition is opposite to the one of p-type semiconductor 29. Theoretically, the larger the carrier densities, the greater the conductivity of passive film, the worse the corrosion resistance 30. The shallow acceptor density is almost three times as much as the donor density, based on the results presented in Table 2, which can be attributed to the higher doping density and the worse degree of order of passive film at region II, it causes the worse the corrosion resistance of passive film. Thus, it causes the decrease of the stability of passive film on 17-4 stainless steel coupled with C110 carbon steel. Based on above mentioned, the results are strongly in agreement with the results of EIS, shown in Figures 3-5. Thus, the potential of (17-4)-C110 couple decrease (as Figure 1).

4. CONCLUSION

In this work, the corrosion of 17-4 stainless steel in the SC couple was studied by electrochemical experiments, i.e., open circuit potential, galvanic potential, electrochemical impedance

spectroscopy and Mott-Schottky curves. 17-4 stainless steel acted as cathode when it coupled with C110 carbon steel. Although there is a huge potential difference between them (0.47V), the galvanic potential of (17-4)-C110 couple at Sc:Sa =1 is almost overlapping with the OCP of C110 carbon steel. Besides, the galvanic potential increases with the increase of Sc:Sa. In the potential range of -1.1 V to -0.3 V, the film formed on 17-4 stainless steel presents as p-type semiconductor because of the p-type semiconductor character of chromium oxide in bi-layer structure. Due to a strong cathodic polarization on 17-4 stainless steel when it coupled with C110 carbon steel, the stability and integrity of passive film on 17-4 stainless steel decreases. Thus, a decrease in corrosion resistance of 17-4 stainless steel over time can be found.

ACKNOWLEDGEMENTS
The authors thank for the financial support of National Natural Science Foundation of China (51501160) and PLN1308 of State Key Laboratory of Oil and Gas Reservoir Geology and Exploitation (Southwest Petroleum University).

References

1. E. Bardal, Corrosion and Protection, Springer, 2004, 94
2. J. R. Vera, S. Hernández, C. Scott and O. Moghissi, Predicting Galvanic CO_2 Corrosion in Oil and Gas Production Systems. NACE Corrosion 20008 Conference & Expo, 2008, Houston, USA, Paper No.08539.
3. C. Q. Ren, M. Zhu, L. Du, J. B. Chen, D. Z. Zeng, J. Y. Hu and T. H. Shi, *Int. J. Electrochem. Sci.*, 10 (2015) 4029.
4. S. Qian and D. Qu, *J. Appl. Electrochem.*, 40 (2010) 247.
5. A. Knudsen, F. Jensen, O. Klinghoffer and T. Skovsgaard, Cost-effective enhancement of durability of concrete structures by intelligent use of stainless steel reinforcement, International conference on corrosion and rehabilitation of reinforced concrete structures. Orlando, Florida, USA, 1998, 1.
6. J. T. Pérez-Quiroz, J. Terán, M. J. Herrera, M. Martínez and J. Genescá, *J. Constr. Steel Res.*, 64 (2008) 1317.
7. J. T. Pérez-Quiroz, E. M. Alonso-Guzmán, W. Martínez-Molina, H. L. Chávez-García, M. Rendón-Belmonte and M. Martínez-Madrid, *Int. J. Electrochem. Sci.*, 9 (2014) 6734.
8. C. F. Dong, K. Xiao, X. G. Li and Y. F. Cheng, *Wear*, 270 (2010) 39.
9. W. Y. Wu, S. S. Hu and J. Q. Shen, *Mater. Design*, 65 (2015) 855.
10. C. F. Dong, K. Xiao, X. G. Li and Y. F. Cheng, *J. Mater. Eng. Perform.*, 20 (2011) 1631.
11. C. Q. Ren, D. Z. Zeng, J. H. Lin, T. H. Shi and W. G. Chen, *Ind. Eng. Chem. Res.*, 51 (2012) 4894.
12. A. Romaine, M. Jeannin, R. Sabot, S. Necib and P. Refait, *Electrochim. Acta.*, 182 (2015) 1019.
13. K. Fushimi, A. Naganuma, K. Azumi and Y. Kawahara, *Corros. Sci.*, 50 (2008) 903.
14. X. K. Zhong, S. Y. Yu, L. J. Chen, J. Y. Hu and Z. Zhang, *J. Mater. Sci.: Mater. Electron.*, 28 (2017) 2279.
15. J. Wolstenholme, *Corros. Sci.*, 13 (1973) 521.
16. X. K. Zhong, L. J. Chen, B. Medgyes, Z. Zhang, S. J. Gao and L. Jakab, *RSC Adv.*, 7 (2017) 28186.
17. X. W. Chen, J. H. Wu, J. Wang and C. L. Wang, *Corros. Sci. & Prot. Technol.*, 22 (2010) 363.
18. D. D. Macdonald, *Electrochim. Acta.*, 56 (2011) 1761.
19. C. S. Enache, J. Schoonman and R. van Krol, *J. Electroceram.*, 13 (2004) 177.

20. G. Goodlet, S. Faty, S. Cardoso, P. P. Freitas, A. M. P. Simões, M. G. S. Ferreira and M. Da Cunha Belo, *Corros. Sci.*, 46 (2004) 1479.
21. J. Sikora, E. Sikora and D. D. Macdonald, *Electrochim. Acta.*, 45 (2000) 1875.
22. P. Schmuki and H. Böhni, *Electrochim. Acta.*, 40 (1995) 775.
23. J. F. Dewald, *J. Phys. Chem. Solids.*, 14 (1960) 155.
24. L. Pons, M. Délia, R. Basséguy and A. Bergel, *Electrochim. Acta.*, 56 (2011) 2682.
25. M. H. Dean and U. Stimming, *J. Electronal. Chem.*, 228 (1987) 135.
26. S. Ningshen, U. K. Mudali, V. K. Mittal and H. S. Khatak, *Corros. Sci.*, 49 (2007) 481.
27. I. M. Gadala and A. Alfantazi, *Appl. Surf. Sci.*, 357 (2015) 356.
28. N. E. Hakiki, M. Da Cunha Belo, A. M. P. Simões and M. G. S. Ferreira, *J. Electrochem. Soc.*, 145 (1998) 3821.
29. D. G. Li, J. D. Wang, D. R. Chen and P. Liang, *J. Power Sources*, 272 (2014) 448.
30. J. H. Ding, L. Zhang, M. X. Lu, J. Wang, Z. B. Wen and W. H. Hao, *Appl. Surf. Sci.*, 289 (2014) 33.

© 2017 The Authors. Published by ESG (www.electrochemsci.org). This article is an open access article distributed under the terms and conditions of the Creative Commons Attribution license (http://creativecommons.org/licenses/by/4.0/).